Design and Simulation of a Multistable Nano-actuator

Xingxing LIU, Frédéric LAMARQUE, Emmanuel DORE and Christine PRELLE

Université de Technologie de Compiègne
Laboratoire Roberval UMR 7337
Compiègne 60200, Oise, France
{xingxing.liu, frederic.lamarque, emmanuel.dore, christine.prelle}@utc.fr

Abstract—**The design of a monolithic multistable nano-actuator is presented. Then, a mathematical model and a finite element model (FEM) are constructed and compared. This multistable nano-actuator is based on four parallel coupled bistable modules. Each bistable module uses three central clamped bistable buckled beams as the bistable mechanism. In order to have an output at nano-scale, a flexible hinges based stroke reducing structure is integrated for each bistable module. A bistable module has two stable output positions. The four bistable modules are coupled through levers which are connected by flexible hinges in the aim to get sixteen discrete output positions. By appropriate design, these output positions can be linearly distributed over an axis. The designed nano-actuator presented in this work has linearly distributed output positions from 0 to 150nm with a constant step about 10nm.**

Keywords— bistable buckled beam; multistable; nano-actuator; flexible hinge; FEM; monolithic design.

I. INTRODUCTION

At present, Micro electro mechanical system (MEMS) technology trend is reshaping modern micro-devices to achieve smaller dimensions. As a consequence, the integration of power supply modules or external sensors (e.g., position sensor, etc.) in these micro-devices becomes more difficult. One of the solutions to solve this problem is to utilize multistable actuators (or digital actuators). A multistable actuator has several stable output positions that can be controlled using open-loop method, thus, avoiding the need to integrate additional sensors for position control. Furthermore, in these multistable actuators, the stable positions are self-maintained without the need of external input energy, which allow them to only consume energy during the switching cycle. This results in low level power consumption which makes them suitable in special scenarios such as applications in which actuators are not frequently actuated. So, to economize the power consumption, this feature of the multistable actuators can reduce power dependence of the micro devices.

Generally, multistable actuators are based on bistable actuators. By coupling several bistable actuators, a multistable actuator can have 2^n stable positions, where n is the number of bistable modules. Huy-Tuan Pham et al. designed and fabricated a quadristable actuator by serially connecting two bistable modules [1]. This quadristable actuator has four stable positions distributed over a single axis. By connecting two bistable modules in two mutually perpendicular directions, Jeong Sam Han et al. [2] designed a quadristable actuator which has four stable positions: two in x-axis and two in y-axis. Another strategy to get 2D workspace lead Vincent Chalvet et al. [3] to design a planar digital robot by coupling 6 bistable modules in parallel. This device proposes 64 output positions uniformly distributed in a square workspace.

As mentioned, multistable actuators are based on bistable actuators. For a bistable actuator, one of the key characteristics is the bistable mechanism. With the merits of self-stability and big output force, bistable buckled beam became one of the mostly used mechanisms for bistable actuators. Bistable buckled beams can be divided into three groups: pre-compressed beams, pre-shaped beams and pre-stressed beams. A bistable micro-actuator based on pre-compressed buckled beam was designed by Zaidi et al. [4]. In this study, material ABS+ was machined by rapid prototyping technique (3D printer). The bistability was demonstrated but the preload operation was complex and hard to control. In the design of Pane et al. [5] a pre-stressed bistable buckled beam was fabricated by patterning the active silicon (Si) layer of SOI (silicon-on-isolator). The pre-stress was introduced by the difference in thermal expansion between Si and SiO_2 layers during the oxidation process. The preload operation was replaced by pre-stress but the depth of oxidation is also a challenge. Jin et al. [6] designed a bistable actuator based on two central clamped pre-shaped parallel beams using DRIE (deep reactive-ion etching) technique. The pre-shaped beam avoided the preload operation but there is a geometry limit which makes the actuator's stroke much bigger than pre-compressed and pre-stressed bistable beams with the same dimensions. Furthermore, the amplitudes of forces in forward and backward directions are not identical which can be a limit for some applications.

II. PROPOSED DESIGN

Considering the fact that all the systems described in previous section have micrometric resolution, we have decided to go one step forward with a concept of multistable actuator having nanometric resolution. The output resolution was improved through a stroke reduction system integrated into the actuator. The designed multistable actuator is shown in Fig. 1. It is formed by four bistable modules. To combine the outputs of these four bistable modules and get a series of outputs distributed over an axis, the four modules are coupled through a levers based parallel coupling system.

In our design central clamped pre-shaped beams were used as the bistable element in each bistable module. According the

work of Jin et al. [6], two parallel centrally clamped beams are enough to constrain the rotation of the beam at the mid points. But for us, a big force is necessary to drive the reducing system, so three parallel pre-shaped beams are used to increase the force (Fig. 1). They are designed and fabricated to have a cosine shape. The two ends of the beams are fixed with a supporting bracket (Fig. 2). To reduce the stroke, a reducing structure with a big reducing factor is added to each bistable module.
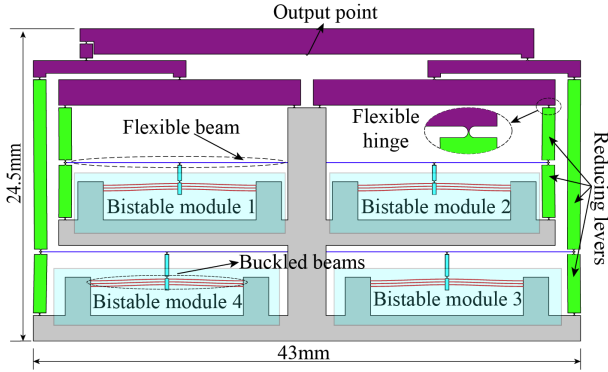
Fig. 1. Multistable nano-actuator

The reducing structure is constructed with flexible beam and levers connected by flexible hinges. Flexible hinges were utilized because of the advantages of no friction, no hysteresis error and can be integrated monolithically [8]. Output displacement of bistable buckled beams will cause the deformation of flexible beam which will lead to a reduced movement of the free end (e.g., the left end of flexible beam for bistable module 1 in Fig. 1) in the direction which is orthogonal to the input direction. Then this movement will cause the rotation of the vertical levers. This rotation will generate a reduced movement. Finally, the direction is changed again to align the output movement in the input direction.

III. MODELING

A. Bistable element

Three central clamped parallel pre-shaped beams are chosen as the bistable element for the bistable module shown in Fig. 2. In a free pre-shaped configuration, as shown in Fig. 3a, the transitional buckling mode is the second buckling mode (an S shape). The Force-Displacement chart for a free pre-shaped beam shows that the force needed to switch the beam from the first extreme position (designed shape) to the second extreme position is always positive (Fig. 3c), i.e. after withdraw the switching force, the beam will recover to the original position. In such a case, the beam is monostable. To overcome this drawback, Jin et al. [6] have proved that clamping two parallel pre-shaped beams at their central points can constraint the rotation of the beams. As shown in Fig. 2, when a moment is applied on the clamping part, internal stress will against the rotation. So the transitional buckling mode will be the third buckling mode shown in Fig. 3b. The third buckling mode can create a higher energy barrier between the two extreme positions. As shown is Fig. 3d, for such a configuration, the switching force has a negative part. That

means the central clamped pre-shaped beam is this time bistable.
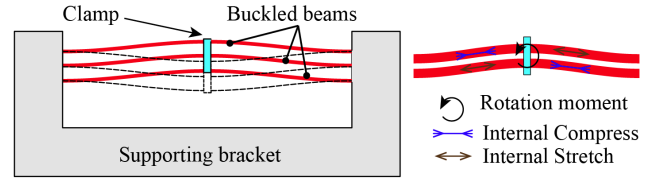
Fig. 2. Bistable module and illustration of constrained rotation at the central points by clamping two parallel beams
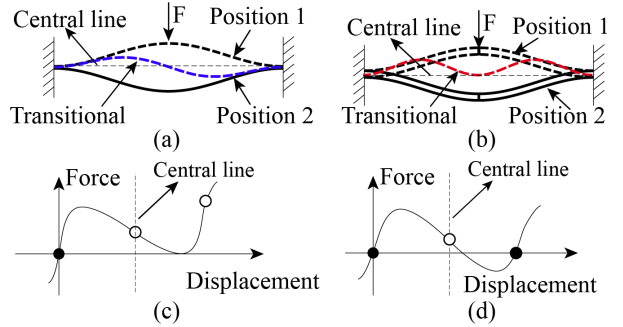
Fig. 3. Pre-shaped beam: (a) Free pre-shaped beam; (b) Central point rotation constrained pre-shaped beam; (c) Force-Displacement chart for (a); (d) Force-Displacement chart for (b).

B. Modeling of a single pre-shaped beam

To quantitatively calculate the force generated by the bistable buckled beams, a coordinate system is constructed for one single beam as shown in Fig. 4.
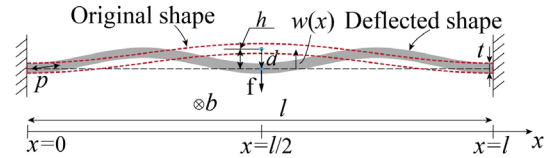
Fig. 4. Model of pre-shaped beam

According to the Euler-Bernoulli beam theory [7], the buckled beam with a length of l, a thickness of t, a depth of b and a central original rise of h satisfies the following equation:

$$EI\frac{d^4w}{dx^4} + p\frac{d^2w}{dx^2} = 0 \qquad (1)$$

Where $w(x)$ is the deflection of the beam, E is the Young's modulus, $I=bt^3/12$ is the inertia moment with respect to the axis of deflection, p is the axial load in the beam, d is the deflected distance of the central point.

During the deflection, the shape of beam can be expressed as a superposition of a set of infinite buckling modes. Using minimum energy principle, the switching force f during the deflection process for central clamped parallel pre-shaped beams can be calculated by following equations [6]:

$$F(\Delta) = \begin{cases} F_1 = \dfrac{3\pi^4 Q^2}{2}\Delta\left(\left(\Delta - \dfrac{3}{2}\right)^2 - \left(\dfrac{1}{4} - \dfrac{4}{3Q^2}\right)\right) & p < p_2 \\[2mm] F_2 = 4.18\pi^4 - 2.18\pi^4\Delta & p = p_2 \\[2mm] F_3 = 8\pi^4 - 6\pi^4\Delta & p = p_3 \end{cases} \quad (2)$$

Where $F = fl^3/EIh$ is normalized switching force, $\Delta = d/h$ is the normalized deflection, p_2 and p_3 are the critical axial load for buckling mode 2 and mode 3. $Q = h/t$ is a geometry factor. The beam is bistable only when $Q \geq 2.31$. The bigger Q is the more bistable the beam will be. The chart of switching force versus displacement is calculated and shown in Fig. 5.
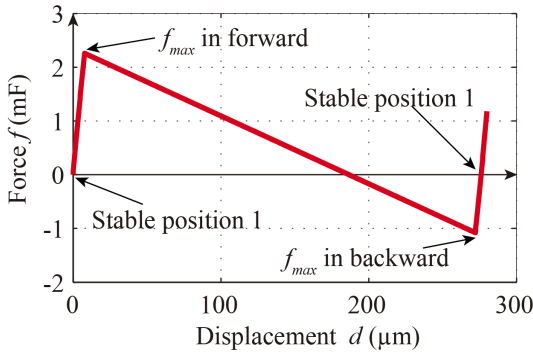
Fig. 5. Force-Displacement chart for central clamped pre-shaped beam
(E=112Gpa, t=20μm, h=140μm, b=0.5mm, l=12mm)

C. Reducing structure

In [6], it is reported that when the geometry factor Q is bigger than 6, central clamped pre-shaped beams will be well bistabled. But for a given length l, bigger Q will create bigger internal stress. So to avoid enlarging the length of beam too much and have the beam well bistabled, Q is chosen to be 7. Then with a given thickness of beam $t=20\mu m$, the central original rise $h=Q\cdot t$ will be $140\mu m$ and the stroke is about two times of h, i.e. $280\mu m$. Obviously the stroke is too big for a nano-actuator, then a flexible hinges based stroke reducing structure is monolithically integrated. The bistable module 1 is taken as an example and shown in Fig. 6a.
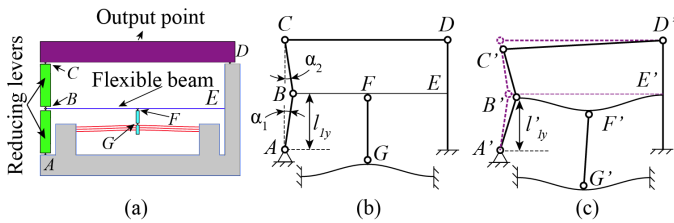
Fig. 6. Flexible hinges based stroke reducing structure: (a) Bistable module 1;
(b) Schematic of reducing structure; (c) Actuated reducing structure.

In Fig. 6a, A, B, C, D, F and G are circular flexible hinges (a zoomed hinge can be seen in Fig. 1). If we consider the flexible hinges as frictionless rotational hinges, the bistable module 1 can be simplified to the schematic shown in Fig. 6b. The specific reducing factor depends a lot on the original angles between AB and BC with respect to the vertical

direction, i.e. α_1 and α_2 (Fig. 6b). The smaller the angle is the bigger the reducing factor will be.

In previous work [10], the reducing structure has some unwanted output behavior (Fig. 7). When the bistable element is switched between two stable positions, it will generate an approximate square wave input for the reducing structure. But the output is not a square like wave. When it started from stable position 1 to stable position 2, the output would go to the inverse direction for a small distance, then turned back to the stable position 2. Similar case happened when it came back to position 1. This cause the output of switching process inconsistent. If we consider the lever AB and rotate it from AB to AB' (Fig. 7), the trace of B is an arc. So the component movement in vertical direction, i.e., the output, will firstly increase then decrease. This can explain the unwanted part in output. So, to avoid the problem, trace of B should not pass the vertical line where the maximum output occurs. Furthermore, when the beam BE is deflected, a force with the same direction will apply on BA and this force will cause a small elastic deformation of BA. In our case, BA will be compressed. So, BA becomes shorter. This deformation is much smaller than the output of B, but it will be added directly to the final output without reduction effect. So, when it is compared to the final output it will cause a visible change on the output behavior. When this elastic deformation happens in the opposite direction, it can cause the same unwanted behavior shown in Fig. 7.
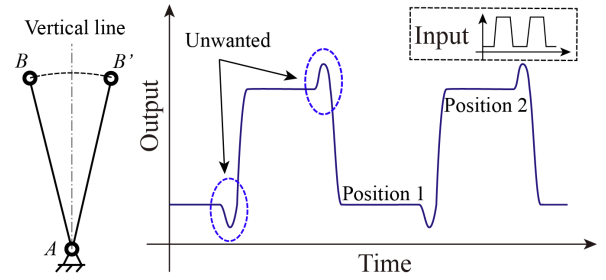
Fig. 7. Illustration of the unwanted behavior in output.

In our case, the bistable beams are originally designed to be upward buckled, so that when the bistable beams are switched to the other stable position, the force in lever GF, which connect bistable beams and the reducing structure, is always tensile force. This will assure that GF will not be twisted due to flexible hinges G and F. In this configuration, the force applied on AB is in downward direction and will cause an elastic deformation in the same direction. As the deflection of beam BE will always generate a movement of B towards the right side, the original position of AB is chosen on the right side of the vertical line, in order to make the output in the same direction with the elastic deformation.

D. Calculation of Reducing Factor

The first reducing level is the flexible beam shown in Fig. 8. It can be considered as a frictionless supported cantilever. It is obvious that the deflected shape is symmetrical with respect to the mid-point. If we define the force applied to the mid-point of the beam as F_d and the length after deflection as l_d, the deflection of the left half part δ_x, $x \in [0, l_d/2]$, can be

calculated by the direct integration method with following equations:
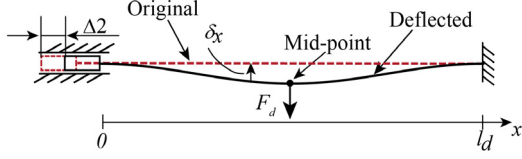
Fig. 8 Flexible beam for the first reducing level

$$M(x) = \frac{F_d}{8EI_d}(l_d - 4x), x \in [0, \frac{l_d}{2}] \tag{3}$$

$$\theta(x) = \int M(x)dx = \frac{F_d}{8EI_d}(l_d x - 2x^2) + C_1, x \in [0, \frac{l_d}{2}] \tag{4}$$

$$\delta_x = \int \theta(x)dx = \frac{F_d}{8EI_d}\left(\frac{l_d x^2}{2} - \frac{2}{3}x^3\right) + C_1 x + C_2, x \in [0, \frac{l_d}{2}] \tag{5}$$

Where $M(x)$ is the internal moment, θ_x is the rotation at x. E is the elastic module, $I_d = bt_d^3/12$ is the inertia moment with respect to the axis of deflection, t_d is the thickness of the flexible beam. C_1 and C_2 are constants for integral. With the fact that both the rotation θ and deflection δ are zero at $x=0$, we know that $C_1=C_2=0$. So the deflection at mid point is:

$$\delta_{\frac{1}{2}l_d} = \frac{F_d l_d^3}{192 EI_d} \tag{6}$$

If we define the stroke of bistable beams as Δ_1, then:

$$\Delta_1 = \delta_{\frac{1}{2}l_d} = \frac{F_d l_d^3}{192 EI_d} \tag{7}$$

$$F_d = \frac{192 \Delta_1 EI_d}{l_d^3} \tag{8}$$

Then the arc length s (the length before deflection) of the flexible beam is:

$$s = 2\int_0^{\frac{l_d}{2}} \sqrt{1 + \left(\frac{d\delta_x}{dx}\right)^2} dx$$

$$= \frac{1}{4EI_d}\int_0^{\frac{l_d}{2}} \sqrt{F_d^2 x^2 (l_d - 2x)^2 + 64E^2 I^2} dx \tag{9}$$

$$= 2\int_0^{\frac{l_d}{2}} \sqrt{576\Delta_1^2 x^2 (l_d - 2x)^2 + 1} dx$$

The output of the flexible beam is the movement of the left end Δ_2:

$$\Delta_2 = s - l_d \tag{10}$$

So the reducing factor of first reducing level R_1 is:

$$R_1 = \frac{\Delta_1}{\Delta_2} \tag{11}$$

The second reducing level is accomplished by levers (*AB* and *BC* in Fig. 6) connected with flexible hinges. The output of the deflected flexible beam Δ_2 is the input for the second

reducing level. Δ_2 will cause the rotation of *AB* and *BC*. If we define the length of *AB* as l_1 and the vertical component of l_1 as l_{1y}, then:

$$l_{1y} = l_1 \cos\alpha_1 \tag{12}$$

The vertical component, after *AB* is rotated, l'_{1y} is:

$$l'_{1y} = \sqrt{l_1^2 - (l_1 \sin\alpha_1 + \Delta_2)^2} \tag{13}$$

Similarly we define the length of *BC* as l_2, then:

$$l_{2y} = l_2 \cos\alpha_2 \tag{14}$$

$$l'_{2y} = \sqrt{l_2^2 - (l_2 \sin\alpha_2 + \Delta_2)^2} \tag{15}$$

The output Δ_3 for the second reducing level is:

$$\Delta_3 = (l_{1y} - l'_{1y}) + (l_{2y} - l'_{2y}) \tag{16}$$

Then we come to the third reducing level. Since the output is taken from the mid-point of *CD*, it will be half of Δ_3. The total reducing factor R_{M1} for bistable module 1 is:

$$R_{M1} = \frac{2\Delta_1}{\Delta_3} \tag{17}$$

The reducing factors R_{M2}, R_{M3} and R_{M4} for other three bistable modules can be calculated with the same process.

E. Coupling the four bistable modules

To form a multistable actuator, the outputs of bistable modules should be coupled. There are two kinds of coupling strategies: serial coupling (Fig. 9a) and parallel coupling (Fig. 9b). Serial coupling is simple. The output of module 1 is directly linked to module 2. When module 1 is actuated the whole module 2 will act as the load for module 1. Different from serial coupling, in parallel coupling, two bistable modules are at the same level and they are coupled through coupling structure. The coupling structure in miniature design is normally levers connected by flexible hinges which is a lighter load. At the same time, the coupling structure has a stroke reducing effect. Like it is shown in Fig. 9b, the final output is the weighted average of output 1 and 2.
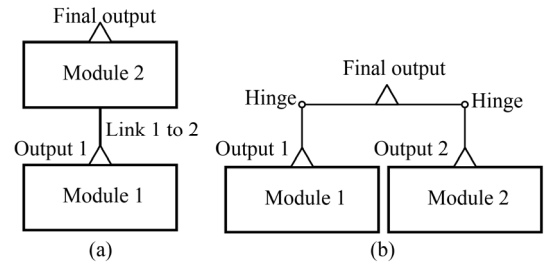
Fig. 9. Coupling strategies: (a) Serial coupling; (b) Parallel coupling

In our design, each bistable module has a reducing structure with relatively weak output stiffness. If serial coupling strategy is exploited, when pre-module (e.g., module 1 in Fig. 9a) drives the whole following module (e.g., module 2 in Fig. 9a), there is the risk that the reducing structure of pre-module could be broken. Therefore, the parallel coupling strategy was chosen (Fig. 10). Furthermore, in parallel

strategy, coupling structure gives an additional reducing effect.

In order to have linearly distributed output positions over an axis, the four bistable modules are designed to have binary changed outputs, e.g., 10nm, 20nm, 40nm and 80. Then the combined outputs could be 10nm, 20nm, 30nm...150nm. Therefore, the reducing factor for the module which has smaller output (Here is module 1 and 2) should be bigger. So the output point L of lever *HI* is nearer to *H* than *I*. Similar case with lever *JK*.
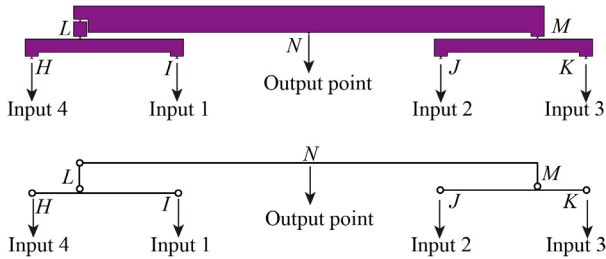
Fig. 10. Parallel coupling structure used in this design (upper part) and simplified schematic (lower part).

IV. SIMULATION AND COMPARISON

A. Stress Verification

The designed multistable nano-actuator is expected to be fabricated on silicon wafer in the future. Since it is a monolithic structure and the flexible parts are expected to be deformed elastically, it should be assured that the internal stress generated during the actuation would not pass the elastic limit of silicon material. Fig. 11a, b and c shows the stress simulated when all four bistable modules are actuated. The elastic limit of silicon has been chosen at 120MPa. The simulation reported a global maximum stress of 81MPa. The position where the maximum stress occurs corresponds to the hinge *B*. In fact, as we see in Fig. 11b, there are two flexible hinges at *B*. These two hinges were utilized to share the deformation at *B*, so that the maximum stress can be reduced.
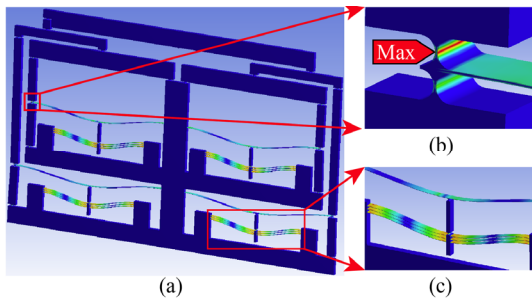
Fig.11. Stress simulation for the multistable nano-actuator: (a) The global result; (b) Location of global maximum stress; (c) Stress of one bistable module. (The deformation is enlarged four time of the real scale)

B. Simulation of bistable module

The forces of bistable modules are analyzed in FEM software. The forces from mathematical model and FEM model for bistable module 4 are shown in Fig. 12. We can see that these two results are quite close to each other except the part near the two peaks. The difference between them is due to the simplification in the mathematical model. As a matter of

fact, in the mathematical model, only the first three buckling modes are considered because the influence of higher buckling modes is relatively small as compared to the first three ones. In FEM analysis, the nonlinear method is used. It is closer to the real behavior of buckling beam. So in the following section the simulation results will be used to decide the reducing factor and get the expected outputs.
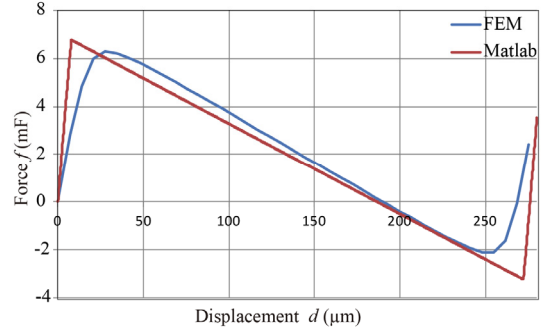
Fig.12. Comparison of mathematic model and FEM model for switching force

C. Simulation of reducing structure

The outputs of the multistable nano-actuator are simulated in FEM software and compared with mathematical model (TABLE I). The results shown here correspond to the situation when only one of the four bistable modules is actuated. Firstly, we found that the biggest difference between two models reached 4.4% which is unacceptable for an accurate model. After carefully analyzing, it was found that the values α1 and α2 (coming from Computer Aided Design model) used for FEM analysis were slightly bigger than the ones used in mathematical model. That is why the FEM analyzing results are always bigger that the mathematical model. As we see in TABLE I, after correcting the angle values, the difference between the two models are quite close to each other, it is less than 1% except for bistable module 4. This big difference for module 4 is caused by the elastic deformation of output lever and it can be reduced by strengthening the output lever.

Then, by properly actuating the four bistable modules, we can get linearly distributed outputs over an axis from about 10nm (10.3 nm in real) to 150nm (154.6 nm in real).

TABLE I. OUTPUT OF FOUR BISTABLE MODULES

	Module 1	Module 2	Module 3	Module 4
Stroke (μm)	275.4	275.4	275.4	275.4
Output of mathematical model before angle correction(nm)	10	20	40	80
Output of mathematical model after angle correction(nm)	10.3	20.7	41.6	83.3
Output of FEM (nm)	10.3	20.7	41.8	81.7
Difference before angle correction (%)	3.2	3.7	4.4	2.1
Difference after angle correction (%)	-0.1	0.1	0.4	-2

V. CONCLUSION

A multistable nano-actuator was designed and analyzed. Mathematical model was constructed to support the design. Furthermore, the designed actuator is analyzed in FEM software. The FEM simulation results are in good agreement with the mathematical model. The actuator has 16 uniformly distributed output positions from 0nm to 150nm with a constant step of 10nm between two positions. As future work, this design will be first fabricated on silicon wafer and second experimentally evaluated.

REFERENCES

[1] Huy-Tuan Pham, Dung-An Wang, "A quadristable compliant mechanism with a bistable structure embedded in a surrounding beam structure," Sensors and Actuators A 167 (2011) 438–448

[2] Jeong Sam Han, Claas Müller, Ulrike Wallrabe, Jan G. Korvink, "Design, simulation, and fabrication of a quadstable monolithic mechanism with x- and y-directional bistable curved beams," *Transaction of the ASME,* vol. 129, pp. 1198-1203, 2007.

[3] Vincent Chalvet, Artur Zarzycki, Yassine Haddab and Philippe Lutz, "Digital Microrobotics Based on Bistable Modules: Design of a non-redundant digital micropositioning robot," IEEE International Conference on Robotics and Automation, Shanghai: China (2011).

[4] Zaidi S., Lamarque F., Favergeon J., Carton O. and Prelle C., Wavelength selective shape memory alloy for wireless micro-actuation of a bistable curved-beam, IEEE Transactions on Industrial Electronics,Vol 58, n°12,pp.5288-5295 (Dec 2011).

[5] I.Z. Pane and T. Asano, "Analysis and fabrication of ampere-force actuated bistable curved beam," Japanese Journal of Applied Physics, vol. 48, pp. 06FK08:1-06FK08:4, 2009.

[6] JIN Qiu, J.H. Lang, and A.H. Slocum, "A curved-beam bistable mechanism," Journal of Micro electro mechanical Systems, vol. 13, pp. 137-145, 2004.

[7] Timoshenko, S. P., and Gere, J. M., 1961, Theory of Elastic Stability, 2nd ed.,McGraw-Hill, New York.

[8] LIU Wei, "Computer aided calculation of angle stiffness of single axis flexible hinge ",Changchun Institute of Op tics, Fine Mechanics and Physics, Chinese Academy of Sciences, Changchun 130021, China

[9] QIN Yu, FENG Zhi-jing, "Simulation and Experiment of Nano-positioning Compliant Mechanism for Motion Reduction", Nanotechnology and Precision Engineering, vol. 5, No. 1, Mar, 2007.

[10] Liu X., Lamarque F., Doré E., Petit L., Pouille P., Duhamel Y., "A bistable micro-actuator with stroke reducing structure," Proceedings of the ASME 2014 12th Biennial Conference on Engineering Systems Design and Analysis (ESDA2014), June 25-27, 2014, Copenhagen, Denmark.